

Theoretical description of pressure- and temperature-induced structural phase transition mechanisms of nitrogen

Hannelore Katzke^{1,*} and Pierre Tolédano²

¹*Institute of Geosciences, Crystallography, University of Kiel, Olshausenstraße 40, 24098 Kiel, Germany*

²*Department of Physics, Faculty of Sciences, University of Picardie, 33 rue Saint-Leu, 80000 Amiens, France*

(Received 4 March 2008; revised manuscript received 26 May 2008; published 5 August 2008)

A theoretical description is proposed for the pressure- and temperature-induced structural transitions of nitrogen. Three regions of the phase diagram are distinguished corresponding to different types of transition mechanisms and parent structures. Combined ordering and displacive reconstructive transitions are found in the lowest-pressure region, from the parent disordered β structure to the ordered α and γ structures. In a second region, which extends from about 2 to 140 GPa at room temperature, group-subgroup related structures occur, which realize ferroelastic or ferroelectric distortions of the δ parent structure. Space-group symmetries, consistent with the assumed structural mechanisms, are proposed for the δ_{loc} , ζ , κ , ι , and θ molecular phases. Above 140 GPa, in the molecular dissociation region, the local structure of the η phase is assumed to realize a link between the molecular ζ and κ phases and the high-temperature cubic-gauche (cg)-N phase. An analogy is pointed out between the amorphous η to superhard cg-N transition and the mixed vortex state to superconducting transition of type II superconductors.

DOI: 10.1103/PhysRevB.78.064103

PACS number(s): 62.50.-p

I. INTRODUCTION

Nitrogen has a complex temperature-pressure phase diagram with a wealth of solid phases, both molecular and non-molecular, with widely different types of intermolecular interactions, crystal structures, and chemical bonds. Therefore, a large variety of structural transition mechanisms are involved between the different phases, which combine orientational order-disorder and displacive processes, showing either reconstructive or weakly first-order and even second-order characters. In this respect, three regions of the phase diagram can be distinguished: below about 2 GPa (region 1) the transitions between the disordered β and ordered α and γ molecular phases are of the reconstructive type, with a loss of group-subgroup relationship between the phase symmetries.^{1,2} Reconstructive structural mechanisms also occur across the transition lines leading above 2 GPa to the δ , δ_{loc} , and ϵ phases.^{3,4} These phases belong to a second region of the phase diagram (region 2), which extends up to about 140 GPa at room temperature, into which not less than seven different phases, denoted δ , δ_{loc} , ϵ , ζ , κ , ι , and θ , have been identified.³⁻⁹ Although only the δ and ϵ structures are known with some accuracy, different experimental observations show that all the phases in region 2 display closely related molecular structures separated by first- or second-order transition lines which preserve a group-subgroup relationship between adjacent structures. Here the transition mechanisms can be described in terms of slight modifications in the ordering and displacements of N_2 molecules. Further compression and temperature increase yield a third region (region 3) of the phase diagram corresponding to a dissociation of the N_2 molecules and observation of two reported nonmolecular structures:⁸⁻¹⁵ the η phase, which is obtained either from the ζ phase or from the room-temperature κ phase, and the high-temperature “polymeric” cubic-gauche (cg) phase.

The phase diagram of nitrogen is shown in Fig. 1. Space-group symmetries are indicated for only six among the 12

solid phases reported experimentally, namely, for the α , β , γ , δ , ϵ , and cg phases, for which a reasonable agreement has been reached on the corresponding structures. In contrast there are insufficient or ambiguous observations concerning the structures of the δ_{loc} , ζ , κ , ι , and θ molecular phases and on the nature of the nonmolecular η phase. In the present paper these phases are inserted into a theoretical description of the structural transition mechanisms occurring in the different regions of the phase diagram of nitrogen. It allows us to propose structural models for the δ_{loc} , ζ , and κ phases, as well as possible structural symmetries for the ι and θ phases. The proposed local structure of the amorphous η phase is assumed to establish a structural link between the molecular ζ or κ structures and the cg-N structure.

Our theoretical description of the transition mechanisms combines different types of considerations which depend on the nature of the transition. For reconstructive transitions the structural mechanisms proceed via a substructure common to the neighboring (group-subgroup unrelated) structures and

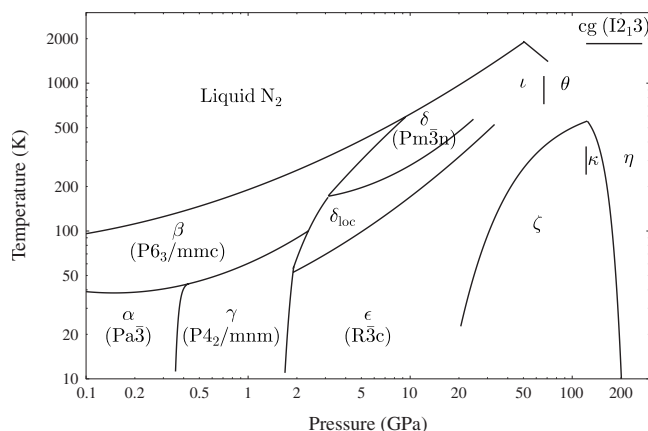


FIG. 1. Temperature-pressure phase diagram of nitrogen from Refs. 1, 8, 9, 12, 15, 22, 26, and 28.

different transition paths can be *a priori* proposed. A Landau-type approach is first used consisting of a group-theoretical analysis which determines the different possible intermediate substructures and verifies that they coincide with absolute minima of the corresponding Landau free energies. The transition path involving the shortest set of displacements and orientations of the molecules and the smaller spontaneous strains is then selected, taking into account the real positions and orientations of the N₂ molecules, assuming implicitly a minimal energy principle for the actual transition mechanism. We finally verify that the selected path is compatible with the respective orientations between neighboring structures and with the full set of available experimental observations. The procedure used for determining the transition mechanisms in region 2 is more direct, since a group-subgroup relationship between the observed structures can be assumed and one has mainly to verify the consistency of the structures which result from our theoretical procedure with the available diffraction and vibration spectra as well as with other eventual observations, such as the volume and density changes and transition order. A more detailed description of our theoretical approach is given in Appendix.

The paper is organized as follows: in Sec. II our proposed structural transition mechanisms are described for the different regions of the phase diagram of nitrogen. Our results are discussed in Sec. III, in connection with the evolution of the molecular interactions under pressure and temperature.

II. STRUCTURAL TRANSITION MECHANISMS IN NITROGEN

A. Region 1: The $\beta \leftrightarrow \alpha$, $\beta \leftrightarrow \gamma$, and $\alpha \leftrightarrow \gamma$ transitions

At 0.1 MPa and between 35.6 K and the melting point at 63.15 K nitrogen has the hcp β structure, which extends along the melting curve up to the β - δ liquid triple point, reached at about 9 GPa and 555–578 K.¹⁶ Below 0.4 GPa the β phase transforms at low temperature to the cubic α phase, whereas at higher pressure, up to 2 GPa, it transforms to the tetragonal γ phase.² The triple α - β - γ point is found at 44.5 K and 0.46 GPa.¹⁷ In the β structure ($P6_3/mmc$, $Z=4$) the N₂ molecules are statically disordered with their molecular axes being tilted from the hexagonal c axis by 54°.¹⁸ The ordered α -N₂ structure ($Pa\bar{3}$, $Z=8$) is characterized by molecular axes oriented along the body diagonals of the cubic unit cell, the molecular centers forming a fcc lattice.¹⁹ In γ -N₂ ($P4_2/mnm$, $Z=4$) the centers of the N₂ molecules form a bct lattice and the molecular axes are directed along the square diagonals of the tetragonal unit cell.²⁰

Figure 2 shows the structural relationship between the α , β , and γ structures. The $\beta \leftrightarrow \alpha$ transition can be described as proceeding via a disordered monoclinic substructure, with $C2/m$ symmetry and $Z=8$ atoms in the conventional C cell [Fig. 2(c)], which is the maximal substructure common to the β structure and to a fcc disordered structure [Fig. 2(b)] from which the α structure derives by orienting the molecules along $\langle 111 \rangle$ directions. The $\beta \rightarrow \alpha$ reconstructive mechanism requires additional antiparallel fractional displacements $\pm \frac{1}{12}[210]_{\beta}$ and a shear deformation e_{xz} decreasing the mono-

clinic angle from 109.471° to 90°. Two different structural paths can be proposed for describing the $\beta \leftrightarrow \gamma$ transformation. It can proceed in two steps, as represented in Fig. 2, across the same $C2/m$ substructure involved in the $\beta \leftrightarrow \alpha$ transition, then through a substructure of higher tetragonal symmetry $I4/mmm$ ($Z=4$) in which the N₂ molecules are statically or dynamically disordered [Fig. 2(e)]. It can also occur with a single intermediate stage, as shown in Fig. 3, via a disordered primitive monoclinic structure ($P2_1/c$, $Z=8$). In addition to the molecular orientation along the square diagonals, the transformation requires antiparallel displacements of the N₂ molecules by $\pm \frac{1}{12}[\bar{1}01]_{\gamma}$ and a shear deformation e_{xz} which decreases the β angle of the primitive monoclinic substructure from 90° to 75.517°. In the same way the $\alpha \rightarrow \gamma$ transformation can proceed either across the disordered $I4/mmm$ structure before reordering into the γ -N₂ structure ($P4_2/mnm$, $Z=4$), as shown in Fig. 2, or go through an ordered monoclinic substructure ($P2_1/c$, $Z=8$), as represented in Fig. 4, with a reorientation of the molecules from the cube to the square diagonals.

B. $\delta \rightarrow \delta_{loc} \rightarrow \epsilon$ transitions

Along the transition lines bounding the β and γ phases above 2 GPa one finds on cooling the δ , δ_{loc} , and ϵ phases. The δ phase has been found below the melt²¹ up to 18 GPa and 900 K and possibly extends up to 50 GPa and 1920 K, at which the melting curve suddenly decreases, suggesting the onset of a phase.²² The cubic unit cell of δ -N₂ ($Pm\bar{3}n$, $Z=16$) is shown in Fig. 5(a). It has a mixed type of disorder,^{4,23,24} the molecules at the vertices and center of the cube lying with equal probability along one of the four body diagonals whereas the other six molecules are disklike disordered. At lower temperature the δ phase undergoes a second-order transition to the δ_{loc} phase.^{5,25} The δ - δ_{loc} transition line has been measured from the β - δ - δ_{loc} triple point, found at about 2.3 GPa and 160 K up to about 21.2 GPa and 456 K.²⁶ δ_{loc} -N₂ occupies on varying pressure a narrow band of almost constant width $\Delta T \approx 110$ K.²⁶

The δ_{loc} structure has been the subject of speculations and is still undetermined. Taking into account the second-order character of the δ - δ_{loc} transition and the property of the δ_{loc} structure to exhibit a partial ordering of the disklike molecules in δ -N₂, as suggested by experimental observations, representing an intermediate stage to the fully ordered lower-temperature ϵ structure, one can propose for δ_{loc} the orthorhombic $Cccm$ structure represented in Fig. 5(b). The corresponding pseudotetragonal C -centered unit cell contains 16 N₂ molecules, with four spherelike molecules disordered over one Wyckoff position $16m$, and 12 disklike molecules disordered over three $16m$ positions. The theoretical argument supporting our proposed δ_{loc} -N₂ structure is that it should be induced by the same order parameter giving rise to the ϵ -N₂ structure from their common parent δ structure. The ordered rhombohedral ϵ structure ($R\bar{3}c$, $Z=16$) shown in Fig. 5(c) is associated with a three-component order parameter of the $Pm\bar{3}n$ space group (see discussion of Table I in Sec. III), corresponding to the shear strains $e_{xz}=e_{yz}=e_{xy}$ which induce

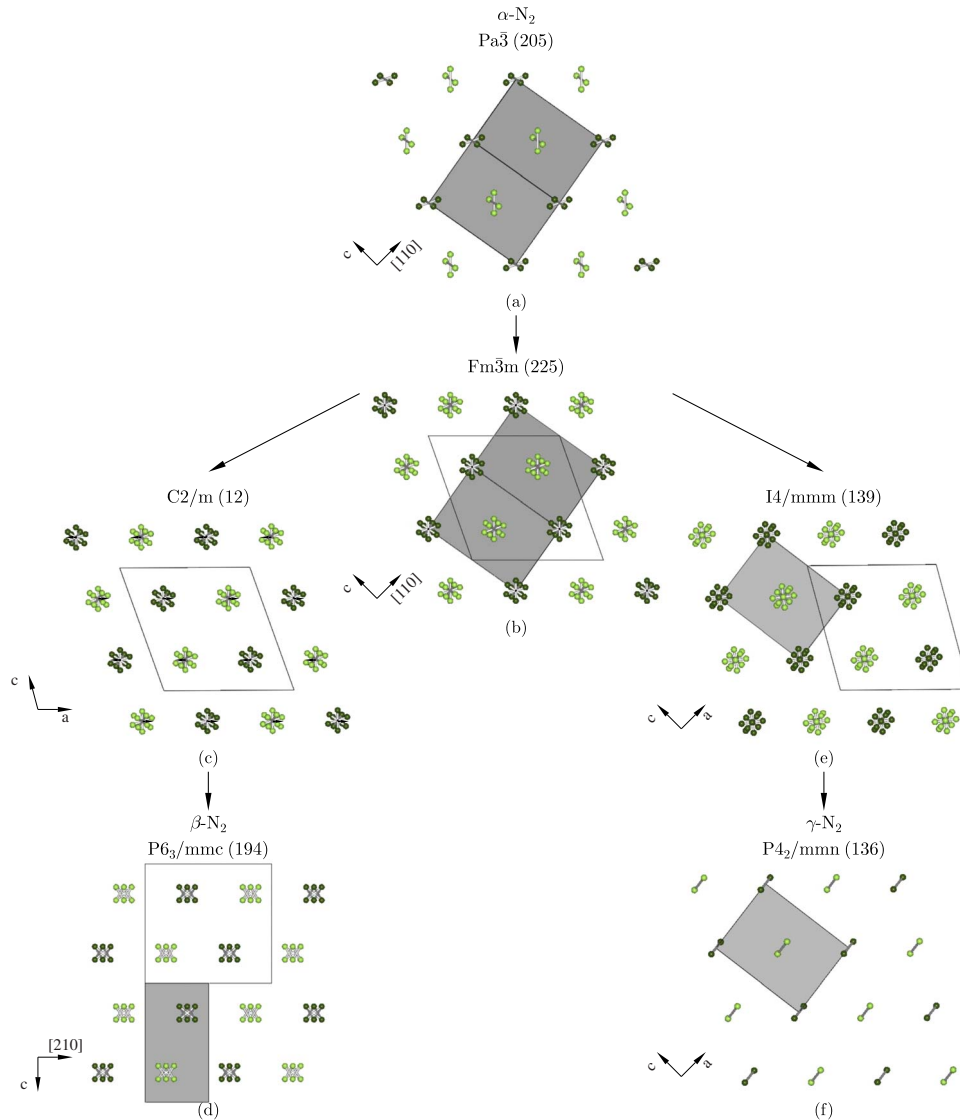


FIG. 2. (Color online) Structural relationship between α -N₂, β -N₂, and γ -N₂. (a) Cubic structure of α -N₂, projected along $[\bar{1}10]$. The cubic unit cell, shown as a gray polyhedron, contains four N₂ molecules centered at the Wyckoff position $4a$ of space group $Pa\bar{3}$ with the nitrogen atoms occupying the Wyckoff position $8c:0.055\ 0.055\ 0.055$. The centers of the N₂ molecules form a fcc lattice in which each molecule points in a different $\langle 111 \rangle$ direction. (b) Static or dynamic disorder of the N₂ molecules increases the symmetry to $Fm\bar{3}m$. The $Fm\bar{3}m$ unit cell, projected along $[\bar{1}10]$, is shown as a gray polyhedron. The unit cell contains four N₂ molecules centered at the Wyckoff position $4a$. The nitrogen atoms occupy one Wyckoff position $32f:1/18\ 1/18\ 1/18$ and one Wyckoff position $24e:\sqrt{3}/18\ 0\ 0$. (c) The α -to- β phase transition can be described as proceeding via a disordered monoclinic substructure with $C2/m$ symmetry common to $Fm\bar{3}m$ and $P6_3/mmc$, with the molecular centers occupying the Wyckoff position $4i:3/4\ 0\ 1/4$ in the disordered α structure and $4i:2/3\ 0\ 1/4$ in the disordered β structure. The monoclinic unit cell with its origin shifted to $p=(0,0,1/2)$ is shown by solid lines. The α -to- β phase transition involves antiparallel displacements of the N₂ molecules and a shear deformation decreasing the monoclinic angle β from 109.471° to 90° . The atomic displacements of $\pm\frac{1}{12}[100]$, corresponding to $\pm\frac{1}{24}[11\bar{2}]$ related to the cubic unit cell of α -N₂ and $\pm\frac{1}{12}[210]$ corresponding to the hexagonal unit cell of β -N₂ are indicated by black arrows of the real magnitude. (d) Hexagonal structure of β -N₂, projected along $[0\bar{1}0]$. The hexagonal unit cell, shown as a gray polyhedron, contains two molecules centered at the Wyckoff position $2d$ with the nitrogen atoms occupying the Wyckoff position $24l:0.2096\ 0.5429\ 0.8053$ of space group $P6_3/mmc$. The molecules are statically disordered with their intramolecular axes tilted from the hexagonal c axis by 54° . (e) The α -to- γ phase transition can be described as proceeding via the same monoclinic $C2/m$ and a latent tetragonal $I4/mmm$ substructure in which the N₂ molecules are statically or dynamically disordered. Ordering of the N₂ molecules decreases the symmetry to $P4_2/mnm$ yielding the structure of γ -N₂ shown in (f). The tetragonal unit cell, shown as a gray polyhedron, contains two molecules centered at the Wyckoff position $2a$ of space group $P4_2/mnm$. The centers of the N₂ molecules form a bct lattice with the intramolecular axes of the molecules directing along the square diagonals of the tetragonal unit cell. The nitrogen atoms occupy the Wyckoff position $4f:0.095\ 0.095\ 0$. Atoms on different heights along $[\bar{1}10]$ in (a) and (b), $[010]$ in (c), $[0\bar{1}0]$ in (d), and $[010]$ in (e) and (f) are shown in different gray shades (colors).

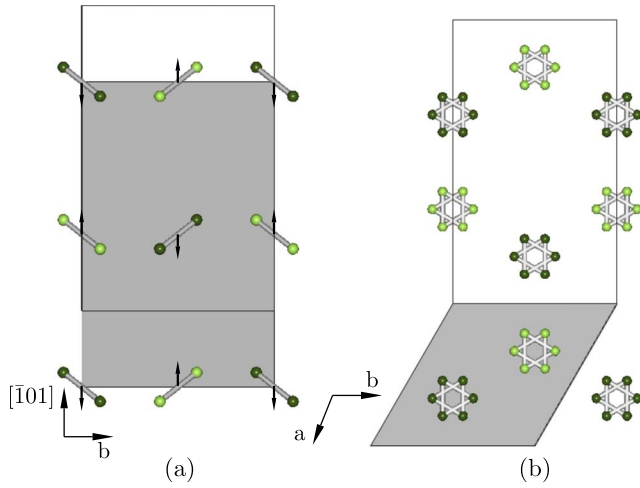


FIG. 3. (Color online) Structural relationship between γ -N₂ and β -N₂. (a) Tetragonal structure of γ -N₂, projected along [101]. The γ -to- β phase transition can be described as proceeding via a common monoclinic substructure ($P2_1/c$, $Z=8$) with the centers of the N₂ molecules occupying the Wyckoff position $4e:3/4\ 0\ 1/4$ in γ -N₂ and $3/4\ 0\ 1/3$ in β -N₂. Therefore, the structure of γ -N₂ is transformed into the structure of β -N₂ by antiparallel displacements of the molecular centers by $\pm\frac{1}{12}[\bar{1}01]$, indicated by black arrows of the real magnitude, and a shear deformation increasing the monoclinic angle β of the common $P2_1/c$ substructure from 75.517° to 90° . The tetragonal unit cell is shown as a gray polyhedron; the monoclinic $P2_1/c$ unit cell of the common substructure is shown by solid lines. The origin is shifted to $p=(1/2,0,0)$. (b) Hexagonal structure of β -N₂, projected along [001]. The hexagonal unit cell is shown as a gray polyhedron, the monoclinic unit cell is shown by solid lines. The N₂ molecules are statically disordered with their intramolecular axes tilted from the hexagonal c axis by 54° . Atoms on different heights along [101] in (a) and [001] in (b) are shown in different gray shades (colors).

a rhombohedral deformation of the cubic unit cell by 4.86° . This imposes a first-order character to the δ - ϵ transition due to the existence in the Landau free energy of the cubic invariant $e_{xz}e_{yz}e_{xy}$. This invariant vanishes at the transition to the assumed $Cccm$ - δ_{loc} structure, since only one order-parameter component (e_{xz}) is nonzero, therefore allowing a second-order δ - δ_{loc} transition. Figure 5 shows the successive ordering mechanisms occurring from the disordered δ -N₂ structure to the ordered ϵ -N₂ structure, in which two molecules at positions $2b$ point along the body diagonals of the rhombohedral unit cell, whereas the other six molecules point in different $\langle 122 \rangle$ directions.

C. From region 1 to region 2: The $\beta \leftrightarrow \delta$, $\beta \leftrightarrow \delta_{loc}$, $\gamma \leftrightarrow \delta_{loc}$, and $\gamma \leftrightarrow \epsilon$ transitions

Between region 1 and region 2 of the phase diagram four different reconstructive transition lines separate the low-pressure β and γ phases from the higher-pressure δ , δ_{loc} , and ϵ phases, the corresponding transition mechanisms proceeding via the same intermediate monoclinic substructure (Cc , $Z=32$) which is common to the β , γ , δ , and ϵ structures. The hexagonal-to-cubic $\beta \leftrightarrow \delta$ transition takes place between the

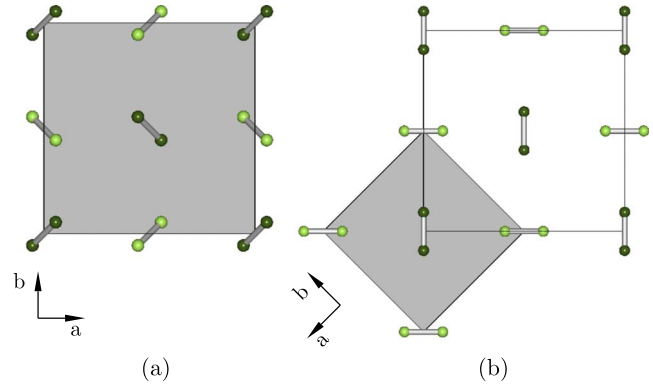


FIG. 4. (Color online) Structural relationship between α -N₂ and γ -N₂. (a) Cubic structure of α -N₂, projected along [001]. The α -to- γ transition can be described as proceeding via a common monoclinic substructure ($P2_1/c$, $Z=8$) with the molecular centers occupying the Wyckoff positions $2a$ and $2d$. The nitrogen atoms occupy two Wyckoff positions $4e:0.055\ 0.055\ 0.055$ and $0.555\ 0.445\ 0.945$ in α -N₂ and $0\ 0\ 0.095$ and $0.5\ 0.405\ 0$ in γ -N₂, respectively. The α -to- γ phase transition involves a reorientation of the N₂ molecules pointing with their intramolecular axes in different $\langle 111 \rangle$ directions in the cubic structure of α -N₂ and along the square diagonals in the tetragonal structure of γ -N₂ shown in (b). The tetragonal unit cell of γ -N₂, projected along $[00\bar{1}]$ contains two molecules centered at the Wyckoff position $2a$ of space group $P4_2/mnm$. The nitrogen atoms are located at the Wyckoff position $4f:0.095\ 0.095\ 0$. The cubic and tetragonal unit cells are shown as gray polyhedra in (a) and (b). The monoclinic unit cell of the common substructure is indicated by solid lines. Its origin is shifted to $p=(1/2,1/2,1/2)$ in (b). Atoms on different heights along [001] in (a) and (b) are shown in different gray shades (colors).

two β - δ - δ_{loc} - and β - δ -liquid triple points.^{7,16,26} The arrows in Fig. 6(a) show the displacive mechanism occurring between the two disordered structures which proceeds via the monoclinic substructure in which the N₂ centers occupy four Wyckoff positions $4a$. The displacements reorder the β spherelike configuration of N₂ molecules into the mixed spherelike and disklike δ configuration shown in Fig. 6(b). The $\beta \leftrightarrow \delta_{loc}$ reconstructive transition takes place between the β - δ - δ_{loc} and β - δ_{loc} - γ triple points,^{7,26,27} the latter being located at about 2.2 GPa and 95 K. It implies with respect to the $\beta \rightarrow \delta$ transition mechanism an additional shear strain e_{xz} which yields the disordered $Cccm$ structure. The $\gamma \leftrightarrow \delta_{loc}$ and $\gamma \leftrightarrow \epsilon$ transitions occur on both sides of the γ - δ_{loc} - ϵ triple point, which has been measured at about 2 GPa and 40 K.²⁶ The $\gamma \rightarrow \delta_{loc}$ and $\gamma \rightarrow \epsilon$ mechanisms, which proceed across their common monoclinic Cc substructure, are described in Fig. 7.

D. Region 2: The $\epsilon \rightarrow \zeta \rightarrow \kappa$ and $\iota \rightarrow \theta$ transitions

At room temperature ϵ -N₂ undergoes with increasing pressure two successive structural changes to molecular structures: one to the ζ phase at about 62 GPa and another one to the κ phase at about 115 GPa.⁸ The $\epsilon \rightarrow \zeta$ transition occurs at low temperature at about 16.5–19 GPa and at 600 K at 125 GPa. Although no volume discontinuity was re-

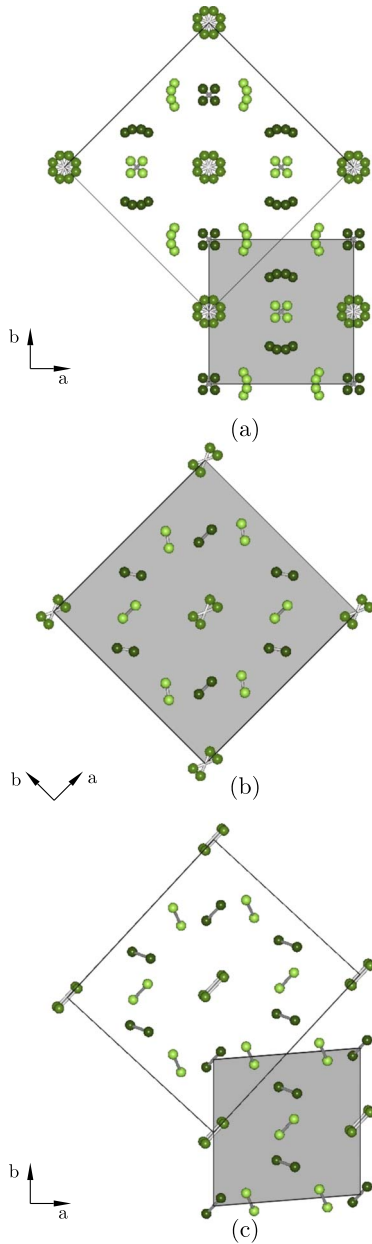


FIG. 5. (Color online) Structural relationship between δ -N₂, δ_{loc} -N₂, and ϵ -N₂. (a) Structure of δ -N₂, projected along [001]. The cubic unit cell, shown as a gray polyhedron, contains eight N₂ molecules centered at the Wyckoff positions $2a$ and $6c$ of space group $Pm\bar{3}n$. The $Cccm$ unit cell of the proposed structure of δ_{loc} -N₂ is represented by solid lines. Its origin is shifted to $p=(0, 1/2, 0)$. (b) Proposed structural model for the partially ordered δ_{loc} phase. The pseudotetragonal unit cell with $a=8.717$ Å and $c=6.164$ Å, shown as a gray polyhedron, contains 16 N₂ molecules. Four spherulike molecules are disordered over one Wyckoff position $16m:0.208$ 0.25 0.042, the other 12 disklike molecules are disordered over three Wyckoff positions $16m:0.9095$ 0.3295 0.0310, 0.1350 0.6040 0.0800, and 0.0555 0.9755 0.2390 in space group $Cccm$. Complete ordering of spherulike and disklike molecules yields the structure of ϵ -N₂, shown in (c). The rhombohedral unit cell, shown as a gray polyhedron, contains eight N₂ molecules centered at the Wyckoff positions $2b$ and $6e$ of space group $R\bar{3}c$. Atoms on different heights along [001] in (a)–(c) are shown in different gray shades (colors).

ported for this transition, the existence of a significant metastability region between the ϵ and ζ phases clearly denotes a first-order character. Volume discontinuity of 2% was measured for the ζ - κ transition, the κ phase being observed on heating up to 800–900 K. Despite a number of proposed symmetries,⁸ the structures of the ζ and κ phases are still unknown. However, the experimental observations suggest that they are group-subgroup related to the ϵ structure, with lower symmetries than ϵ , and a preservation of the number of molecules in the primitive unit cells.⁸ Figure 8 shows our proposed structural models, consistent with the observed diffraction patterns, for the ζ and κ phases and the corresponding structural mechanism for the $\epsilon \rightarrow \zeta \rightarrow \kappa$ sequence of transitions. Thus, a monoclinic symmetry $C2/c$ ($Z=32$) is assumed for the ordered ζ structure shown in Fig. 8(b), with N₂ molecules occupying four Wyckoff positions $8f$. The slight monoclinic deformation, with a β angle close to 90°, is deduced from the ϵ structure by combined strains e_{xz} and $e_{xx}-e_{zz}$ when the ϵ -N₂ rhombohedral angle α reaches 90°. The first-order character of the $\epsilon \rightarrow \zeta$ transition is imposed by the symmetry of the preceding strains which form a cubic invariant in the transition free energy (see Table I). Figure 8(c) represents our proposed structure for the κ phase which is assumed to have the lower monoclinic symmetry $C2$ ($Z=32$), with an occupation of eight Wyckoff positions $4c$ and a monoclinic angle $\beta=91.774^\circ$. The $\zeta \rightarrow \kappa$ transition involves a reorientation of some of the N₂ molecules which breaks the inversion symmetry and creates a dipolar order along the direction of the twofold axis.

Two other molecular high-pressure phases, denoted ι and θ , have been reported at high temperature in region 2 of the phase diagram,⁹ with wide range of stability, including regions where ϵ -N₂ and ζ -N₂ were thought to be the only stable phases of N₂. The ι phase is obtained by heating ϵ -N₂ above 750 K in the range 65–70 GPa, whereas θ -N₂ is observed from 95 to 135 GPa above, respectively, 600 and 1050 K.⁹ The ι phase can be accessed from θ on pressure release at 69 GPa and 850 K. The two structures are still unknown. However, Raman measurements indicate that the ι phase is incompletely ordered and may realize a denser packing of disklike molecules than the δ or δ_{loc} phases. It also shows a lack of inversion center in the ordered θ phase.⁹ Taking into account the location of the two phases in the phase diagram, their presumable connection with the δ , δ_{loc} , and ϵ phases, and using the indexing of their diffraction pattern,⁹ one can tentatively propose a $Ccc2$ ($Z=32$) symmetry for the partly disordered ι structure, corresponding to a direct substructure of our proposed δ_{loc} structure and a $Pnc2$ ($Z=32$) symmetry for the ordered θ structure. More detailed structural data are needed to infer a structural model for the two phases.

E. From region 2 to region 3: The nonmolecular η and cg phases

At room temperature nitrogen exists in molecular form up to 125–150 GPa, at which pressure undergoes a transition to the nonmolecular semiconducting η phase.^{8–12} With decreasing temperature the transition shifts to much higher pressure,

TABLE I. Structural relationships and order-parameter symmetries for the phase transitions observed in nitrogen [column (a)]. Columns (b)–(f) have the following meaning. (b) Relationship between the basic vectors of the conventional unit cells. (c) Multiplication of the number of atoms (or molecules) in the primitive unit cell. (d) Irreducible representations (IRs) associated with the symmetry-breaking mechanisms. The number within brackets is the dimension of the IR which is also the dimension of the transition order parameter. In region 1, from region 1 to region 2, and for the $\zeta \rightarrow \eta$ transition, several IRs are involved at the transitions due to their reconstructive character. The hypothetical substructures induced by each IR are shown in Fig. 10. The notation of the IRs refers to the tables of Stokes and Hatch (Ref. 29) except for $Q_1 = (\frac{\pi}{2a}, \frac{\pi}{b}, \frac{\pi}{c})$ and $F_1 = (\frac{\pi}{2a}, \frac{\pi}{b}, \frac{\pi}{2c})$, which correspond to points located inside the hexagonal and primitive tetragonal Brillouin zones, respectively. (e) Equilibrium values of the order-parameter components (η_i). (f) Secondary order parameters involved at the transitions. (e_{ij}) are components of the strain tensor. P_i are components of the polarization. d_{ij} and L_{ijk} are components of the piezoelectric tensor and of a polar tensor of rank 6, respectively, in the Voigt contracted notation of the indices.

(a)	(b)	(c)	(d)	(e)	(f)
Region 1					
$\beta \rightarrow \alpha$	$\mathbf{a}_\alpha = \mathbf{a}_\beta + \frac{1}{2}(3\mathbf{b}_\beta - \mathbf{c}_\beta)$ $\mathbf{b}_\alpha = \mathbf{a}_\beta - \frac{1}{2}(\mathbf{b}_\beta + \mathbf{c}_\beta)$ $\mathbf{c}_\alpha = -\mathbf{a}_\beta - \frac{1}{2}(\mathbf{b}_\beta + \mathbf{c}_\beta)$	2	Γ_6^+ (2) $+L_3^-$ (8) $+X_5^+$ (6)	$e_{xz}, e_{yz} = 0$ $\eta_1 = \eta_2, \eta_{3 \rightarrow 8} = 0$ $\eta_i = \eta (i = 1-6)$	e_{yz} $e_{xz}, e_{xy} = -e_{yz}$ $L_{113} - L_{112}, L_{166} - L_{155}$
$\beta \rightarrow \gamma$	$\mathbf{a}_\gamma = \frac{1}{2}(2\mathbf{a}_\beta + \mathbf{b}_\beta + \mathbf{c}_\beta)$ $\mathbf{b}_\gamma = \mathbf{b}_\beta$ $\mathbf{c}_\gamma = -\frac{1}{2}(2\mathbf{a}_\beta + \mathbf{b}_\beta - \mathbf{c}_\beta)$	1	Γ_6^+ (2) $+N_2^-$ (4) $+M_4^+$ (1)	$e_{xz}, e_{yz} = 0$ $\eta_1 = \eta_4, \eta_2 = \eta_3 = 0$ η	e_{yz} e_{xz}
$\alpha \rightarrow \gamma$	$\mathbf{a}_\gamma = -\frac{1}{2}(\mathbf{a}_\alpha + \mathbf{b}_\alpha)$ $\mathbf{b}_\gamma = \frac{1}{2}(\mathbf{b}_\alpha - \mathbf{a}_\alpha)$ $\mathbf{c}_\gamma = -\mathbf{c}_\alpha$	$\frac{1}{2}$	Γ_4^+ (3) $+R_1^-$ (4)	$e_{xz}, e_{xy} = e_{yz} = 0$ $\eta_1 = \eta_3, \eta_2 = \eta_4 = 0$	$e_{xy} = e_{yz}$ e_{xz}
Region 1 \rightarrow Region 2					
$\beta \rightarrow \delta$	$\mathbf{a}_\delta = \mathbf{c}_\beta - \mathbf{b}_\beta$ $\mathbf{b}_\delta = \mathbf{c}_\beta + \mathbf{b}_\beta$ $\mathbf{c}_\delta = -(2\mathbf{a}_\beta + \mathbf{b}_\beta)$	4	Q_1 (12) $+ \Gamma_4^-$ (3)	$\eta_1 = \eta_2, \eta_{3 \rightarrow 12} = 0$ $P_x = P_y, P_z$	$e_{xy}, e_{xx} - e_{yy}$ $e_{xy}, e_{xx}, e_{yy}, e_{zz}$
$\gamma \rightarrow \delta_{\text{loc}}$	$\mathbf{a}_{\delta_{\text{loc}}} = 2(\mathbf{a}_\gamma - \mathbf{c}_\gamma)$ $\mathbf{b}_{\delta_{\text{loc}}} = 2\mathbf{b}_\gamma$ $\mathbf{c}_{\delta_{\text{loc}}} = \mathbf{a}_\gamma + \mathbf{c}_\gamma$	4	F_1 (4) $+ \Gamma_4^-$ (3) $+ \Gamma_5^+$ (3)	$\eta_1 = \eta_2, \eta_3 = \eta_4 = 0$ $P_x = -P_y, P_z$ $e_{xz}, e_{xy} = e_{yz} = 0$	$e_{xy}, e_{xx} - e_{yy}$ $e_{xy}, e_{xx}, e_{yy}, e_{zz}$ $e_{xy} = e_{yz}$
$\gamma \rightarrow \epsilon$	$\mathbf{a}_\epsilon = -2\mathbf{b}_\gamma$ $\mathbf{b}_\epsilon = \mathbf{b}_\gamma - 2\mathbf{c}_\gamma$ $\mathbf{c}_\epsilon = 3\mathbf{a}_\gamma - \mathbf{c}_\gamma$	4	F_1 (4) $+ \Gamma_4^-$ (3) $+ \Gamma_5^+$ (3)	$\eta_1 = \eta_2, \eta_3 = \eta_4 = 0$ $P_x = -P_y, P_z$ $e_{xz} = e_{xy} = e_{yz}$	$e_{xy}, e_{xx} - e_{yy}$ $e_{xy}, e_{xx}, e_{yy}, e_{zz}$
Region 2					
$\delta \rightarrow \delta_{\text{loc}}$	$\mathbf{a}_{\delta_{\text{loc}}} = \mathbf{a}_\delta + \mathbf{b}_\delta$ $\mathbf{b}_{\delta_{\text{loc}}} = \mathbf{b}_\delta - \mathbf{a}_\delta$ $\mathbf{c}_{\delta_{\text{loc}}} = \mathbf{c}_\delta$	1	Γ_5^+ (3)	$e_{xz}, e_{xy} = e_{yz} = 0$	
$\delta \rightarrow \epsilon$	$\mathbf{a}_\epsilon = \mathbf{a}_\delta - \mathbf{b}_\delta$ $\mathbf{b}_\epsilon = \mathbf{b}_\delta - \mathbf{c}_\delta$ $\mathbf{c}_\epsilon = \mathbf{a}_\delta + \mathbf{b}_\delta + \mathbf{c}_\delta$	1	Γ_5^+ (3)	$e_{xz} = e_{xy} = e_{yz}$	
$\epsilon \rightarrow \zeta$	$\mathbf{a}_\zeta = \frac{1}{3}(-2\mathbf{a}_\epsilon - \mathbf{b}_\epsilon + 2\mathbf{c}_\epsilon)$ $\mathbf{b}_\zeta = -\mathbf{b}_\epsilon$ $\mathbf{c}_\zeta = \frac{1}{3}(2\mathbf{a}_\epsilon + \mathbf{b}_\epsilon + \mathbf{c}_\epsilon)$	1	Γ_3^+ (2)	$e_{xz}, e_{xx} - e_{zz}$	
$\zeta \rightarrow \kappa$	$\mathbf{a}_\kappa = \mathbf{a}_\zeta, \mathbf{b}_\kappa = \mathbf{b}_\zeta, \mathbf{c}_\kappa = \mathbf{c}_\zeta$	1	Γ_1^- (1)	P_x	
$\delta_{\text{loc}} \rightarrow \iota$	$\mathbf{a}_\iota = \mathbf{a}_{\delta_{\text{loc}}}, \mathbf{b}_\iota = \mathbf{b}_{\delta_{\text{loc}}}, \mathbf{c}_\iota = \mathbf{c}_{\delta_{\text{loc}}}$	1	Γ_2^- (1)	P_x	
$\iota \rightarrow \theta$	$\mathbf{a}_\theta = \mathbf{b}_\iota, \mathbf{b}_\theta = \mathbf{a}_\iota, \mathbf{c}_\theta = -\mathbf{c}_\iota$	2	Y_3 (1)	η	
Region 2 \rightarrow Region 3					
$\kappa \rightarrow \eta$	$\mathbf{a}_\eta = \mathbf{a}_\kappa, \mathbf{b}_\eta = \mathbf{b}_\kappa, \mathbf{c}_\eta = \mathbf{c}_\kappa$	1	Γ_4 (1)	P_x, e_{yz}	
$\zeta \rightarrow \eta$	$\mathbf{a}_\eta = \mathbf{a}_\zeta, \mathbf{b}_\eta = \mathbf{b}_\zeta, \mathbf{c}_\eta = \mathbf{c}_\zeta$	1	Γ_1^- (1) $+ \Gamma_4$ (1)	d_{14}, d_{25}, d_{36}	e_{yz}
Region 3					
$\eta \rightarrow \text{cg}$	$\mathbf{a}_{\text{cg}} = \frac{1}{2}\mathbf{a}_\eta, \mathbf{b}_{\text{cg}} = \frac{1}{2}\mathbf{b}_\eta, \mathbf{c}_{\text{cg}} = \mathbf{c}_\eta$	$\frac{1}{4}$	N_1 (6)	$\eta_1 = \eta_2, \eta_{3 \rightarrow 6} = 0$	$e_{xx} - e_{yy}$ $2\ 2e_{zz} - e_{xx} - e_{yy}$

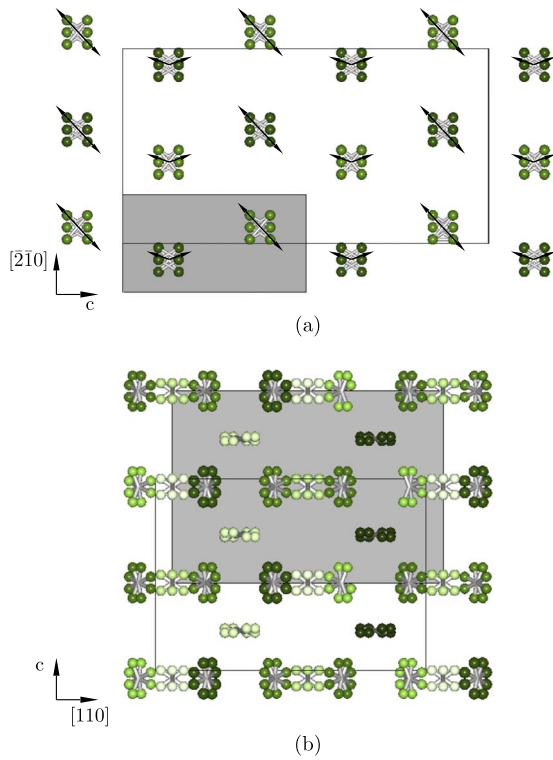


FIG. 6. (Color online) Displacive mechanism associated with the $\beta\text{-N}_2 \rightarrow \delta\text{-N}_2$ phase transition. (a) Hexagonal structure of $\beta\text{-N}_2$, projected along $[010]$. The β -to- δ phase transition can be described as proceeding via a common monoclinic substructure (Cc , $Z=32$) with the N_2 centers occupying four Wyckoff positions $4a$: $1/8$ $1/8$ $11/12$, $1/8$ $5/8$ $11/12$, $3/8$ $3/8$ $1/12$, and $3/8$ $7/8$ $1/12$ in $\beta\text{-N}_2$ and $3/16$ $1/8$ $23/24$, $1/16$ $3/4$ $23/24$, $5/16$ $1/2$ $5/24$, and $7/16$ $7/8$ $23/24$ in $\delta\text{-N}_2$. The hexagonal unit cell is shown as a gray polyhedron, the monoclinic unit cell with its origin shifted to $p=(1/2,0,0)$ is represented by solid lines. The arrows indicate the atomic displacements associated with the structural phase transition. (b) Cubic structure of $\delta\text{-N}_2$, projected along $[\bar{1}10]$. The cubic unit cell, shown as a gray polyhedron, contains eight N_2 molecules centered at the Wyckoff positions $2a$ and $6c$ of space group $Pm\bar{3}n$. The molecules centered at the $2a$ positions are statically disordered with the molecule axes lying with equal probability along one of the four body diagonals yielding a spherelike atomic arrangement. The other six molecules are disordered about the $6c$ positions exhibiting a disklike atomic disorder. Atoms on different heights along $[010]$ in (a) and $[\bar{1}10]$ in (b) are shown in different gray shades (colors).

up to 240–270 GPa, exhibiting a remarkably large hysteresis.^{11,12} Heating at 132 GPa to 2000 K, the η phase transforms into the cg nonmolecular phase with a large volume reduction^{8,15} of about 15%–22%. The transition from the η phase to cg-N is also obtained by direct laser heating of $\zeta\text{-N}_2$ at 120–130 GPa,^{15,28} the cg phase being found above 2000 K and 165 GPa. A number of observations have confirmed the cubic symmetry ($I2_13$, $Z=4$) of the cg-N structure,¹⁴ which corresponds to a covalently single-bonded polymeric network. In contrast, the nature and structure of the η phase is still unclear. It has been depicted^{8–12} either as a single amorphous phase induced by the transformation of the triple-bonded to single-bonded nitrogen molecules as at-

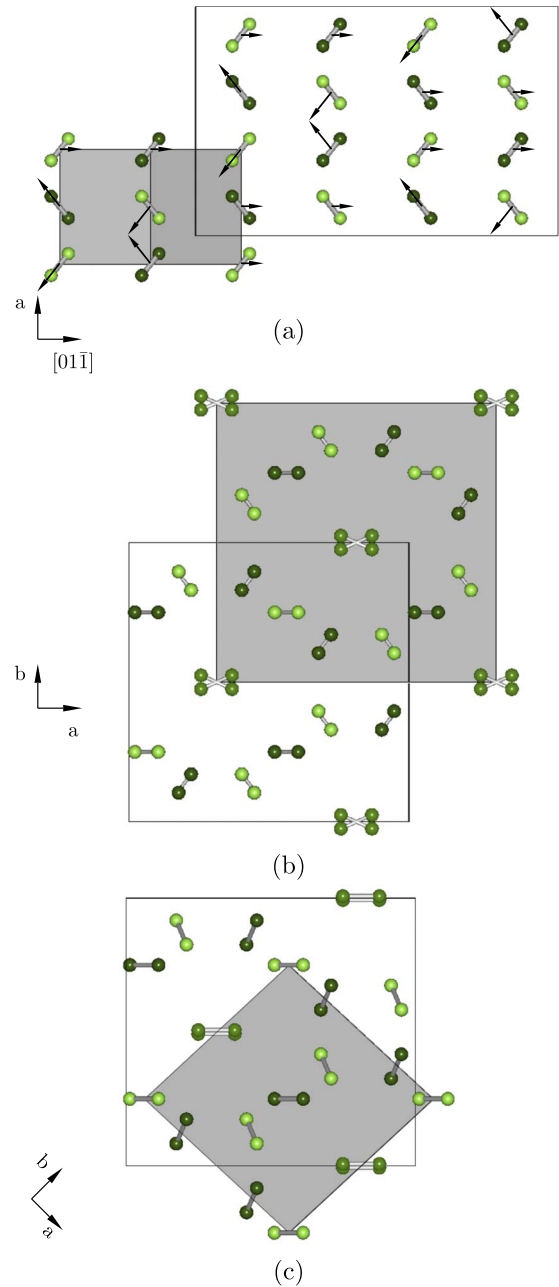


FIG. 7. (Color online) Displacive mechanisms associated with the $\gamma \rightarrow \delta_{\text{loc}}$ and $\gamma \rightarrow \epsilon$ phase transitions. (a) Tetragonal structure of $\gamma\text{-N}_2$, projected along $[01\bar{1}]$. (b) Proposed structure of $\delta_{\text{loc}}\text{-N}_2$, projected along $[001]$. (c) Rhombohedral structure of $\epsilon\text{-N}_2$, projected along $[001]$. The γ -to- δ_{loc} and γ -to- ϵ phase transitions can be described as proceeding via a common monoclinic substructure (Cc , $Z=32$) with the N_2 centers occupying four Wyckoff positions $4a$: $1/8$ $1/8$ 0 , $1/8$ $5/8$ 0 , $3/8$ $3/8$ 0 , and $3/8$ $7/8$ 0 in $\gamma\text{-N}_2$ and $3/16$ $1/8$ $23/24$, $1/16$ $3/4$ $23/24$, $5/16$ $1/2$ $5/24$, and $7/16$ $7/8$ $23/24$ in $\delta_{\text{loc}}\text{-N}_2$ and $\epsilon\text{-N}_2$. The tetragonal, orthorhombic, and rhombohedral unit cells in (a), (b) and (c) are shown as gray polyhedra, the monoclinic unit cells with their origins shifted to $p=(1/4,1/4,-1/4)$ in (a), $p=(-5/16,-1/2,-11/24)$ in (b) and $p=(3/16,-5/16,-11/24)$ in (c) are represented by solid lines. The arrows in (a) indicate the atomic displacements associated with the structural phase transitions. Atoms on different heights along $[011]$ in (a) and $[001]$ in (b) and (c) are shown in different gray shades (colors).

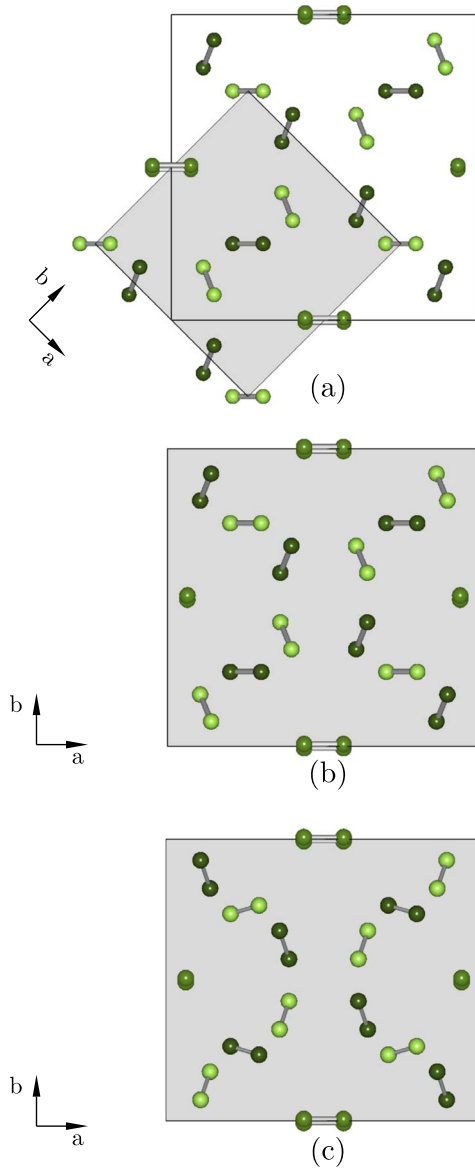


FIG. 8. (Color online) Proposed structural mechanism for the phase sequence $\epsilon\text{-N}_2 \rightarrow \zeta\text{-N}_2 \rightarrow \kappa\text{-N}_2$. (a) Structure of $\epsilon\text{-N}_2$, projected along $[001]$. The rhombohedral unit cell, shown as a gray polyhedron, contains eight N_2 molecules with the nitrogen atoms occupying the Wyckoff position $4c$: 0.0495 0.0495 0.0495 and $12f$: 0.5559 0.2224 0.0701. (b) Proposed structure for $\zeta\text{-N}_2$, projected along $[001]$. $\zeta\text{-N}_2$ is assumed to have a slightly deformed monoclinic structure ($C2/c$, $Z=32$) with $a=6.844$ Å, $b=6.533$ Å, $c=5.148$ Å, and $\beta \approx 90^\circ$. The nitrogen atoms occupy four Wyckoff positions $8f$: 0.2995 0.25 0.0495, 0.3962 0.6739 0.0559, 0.1391 0.9168 0.0701, and 0.0630 0.5071 0.2224. (c) Proposed structure for $\kappa\text{-N}_2$, projected along $[001]$. The ζ -to- κ phase transition is assumed to be the result of a reorientation of some of the N_2 molecules lowering the symmetry to $C2$ ($Z=32$). The proposed structural model for $\kappa\text{-N}_2$ assumes an occupation of eight Wyckoff positions $4c$: 0.4370 0.0071 0.0276, 0.1100 0.0750 0.3201, 0.1400 0.1750 0.1941, 0.2050 0.2650 0.7005, 0.2950 0.2350 0.7995, 0.3600 0.3250 0.3059, 0.3900 0.4250 0.1799, and 0.0630 0.4929 0.4724. The lattice parameters are $a=6.918$ Å, $b=6.202$ Å, $c=4.578$ Å, and $\beta=91.774^\circ$. Atoms on different heights along $[001]$ in (a)–(c) are shown in different gray shades (colors).

tested by Raman and diffraction spectra, or to a strongly disordered phase formed by a fine mixture of different three-coordinated structures involving triple-bonded, double-bonded, and single-bonded nitrogen atoms, or to a heterogeneous region in which the amorphous phase is an extension of the disordered structure with a progressive amorphization process occurring on heating, as suggested by the different colors observed for the sample between room temperature and 2000 K.^{10,28}

Despite the obvious reconstructive character of the $\zeta \rightarrow \eta$ or $\kappa \rightarrow \eta$ transitions which are driven by the destabilization of the triple-bonded nitrogen molecules, one can assume a topological continuity in the sequence of structural mechanisms transforming the $\zeta\text{-N}_2$ or $\kappa\text{-N}_2$ structures into $\eta\text{-N}$ and then into cg-N. Figure 9 shows our proposed $\kappa \rightarrow \eta \rightarrow \text{cg}$ structural sequence. It assumes that the local structure of the η phase is close to the cg structure and realizes a stepwise opening of the $\text{N}\equiv\text{N}$ triple bonds to conjugated $\text{N}=\text{N}-\text{N}=\text{N}$ bonds, as suggested by Lipp *et al.*²⁸ Figure 9(b) shows the local η structure projected along $[001]$ which has the orthorhombic symmetry $C222_1$ with 32 atoms in the conventional C cell, the nitrogen atoms occupying four Wyckoff positions $8c$. The structure involves conjugated shorter (1.285 Å) and longer (1.375 Å) interatomic distances, with coordination number 2. With increasing pressure and temperature further dissociation of N_2 molecules increases the disorder of the orthorhombic structure and completes the amorphization process. Recrystallization occurring above 2000 K yields the covalently bonded cg-N structure. Figure 9(c) shows the structure of the cubic unit cell of the threefold coordinated polymeric nitrogen which contains eight nitrogen atoms at positions $8a$. Note that the bonds in the cg structure are parallel to the molecular axes in $\kappa\text{-N}_2$ and that the calculated displacements from the ϵ to the cg structure are relatively small (≤ 1.37 Å) since they occur in successive steps via the ζ or κ structures.

III. DISCUSSION

Figure 10 shows the structural relationships assumed in our description of the phase transition mechanisms in nitrogen. The irreducible representations (IRs) associated with the corresponding symmetry-breaking mechanisms are indicated along the lines joining the space groups of two successive observed or hypothetical structures. They allow us to determine the order-parameter symmetries and the strain components associated with the transition mechanisms, which are listed in Table I, and to work out the transition free energies which have been used in our approach. Table I also provides the relationships between the basic vectors of the conventional unit cells for neighboring phases, following our proposed mechanisms. Our results can be analyzed in light of the theoretical studies^{2,30–42} which, using a variety of simulation techniques and trial potentials, have attempted to clarify the evolution of the molecular interactions in nitrogen as a function of pressure and temperature. It yields the following picture for the three considered regions of the phase diagram.

In region 1 the strong covalent triple bonds of N_2 molecules coexist with weak van der Waals interactions between

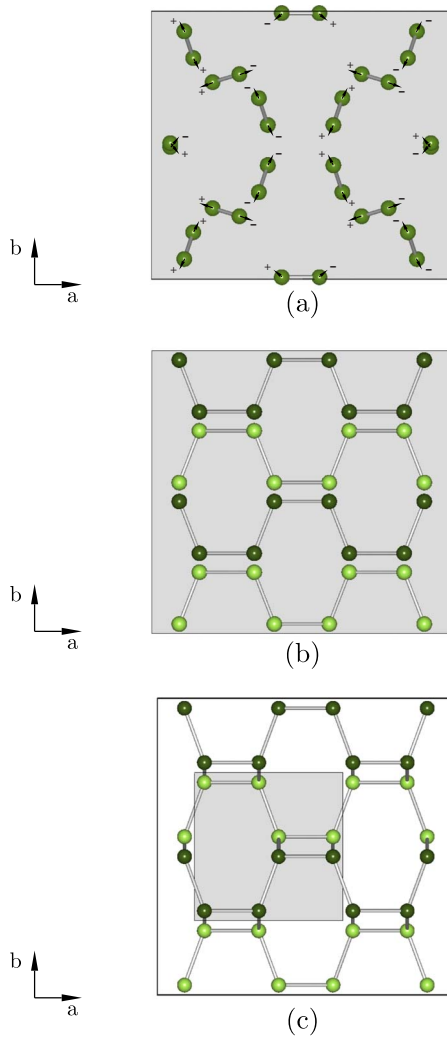


FIG. 9. (Color online) Proposed structural mechanism for the phase sequence $\kappa\text{-N}_2 \rightarrow \eta\text{-N}_2 \rightarrow \text{cg-N}$. (a) Proposed structure for $\kappa\text{-N}_2$, projected along [001]. Arrows indicate the atomic displacements transforming the structure of $\kappa\text{-N}_2$ into the structure of $\eta\text{-N}_2$. (+/-) signs indicate the displacements along [001]. (b) Proposed structure for $\eta\text{-N}_2$, projected along [001]. The structure of $\eta\text{-N}_2$ is assumed to be orthorhombic ($C222_1$, $Z=32$) with $a=6.913$ Å, $b=6.555$ Å, and $c=4.016$ Å. The nitrogen atoms occupy four Wyckoff positions $8c:0.4085$ 0.9665 0.1830 , 0.0915 0.0335 0.6830 , 0.1585 0.2165 0.6830 , and 0.1585 0.2835 0.3170 . The proposed structure of $\eta\text{-N}_2$ can be interpreted as an intermediate phase realizing a stepwise opening of the $\text{N}\equiv\text{N}$ triple bonds to $\text{N}=\text{N}$ double bonds and then to N-N single bonds. In the proposed structure of $\eta\text{-N}_2$ a system of conjugated $-\text{N}=\text{N}-\text{N}=\text{N}-$ bonds is present. (c) Cubic-gauche structure of polymeric nitrogen, projected along [001]. The cubic unit cell, shown as a gray polyhedron, contains eight nitrogen atoms located at the Wyckoff position $8a:0.067$ 0.067 0.067 of space group $I2_13$. Atoms on different heights along [001] in (b) and (c) are shown in different gray shades (colors).

molecules, allowing small oscillations of the center of masses but large orientational oscillations. The orientational degrees of freedom yield the formation below the melt of the disordered close-packed β phase, which is the parent structure in region 1. β transforms on cooling into the α and γ phases across two different types of reconstructive ordering

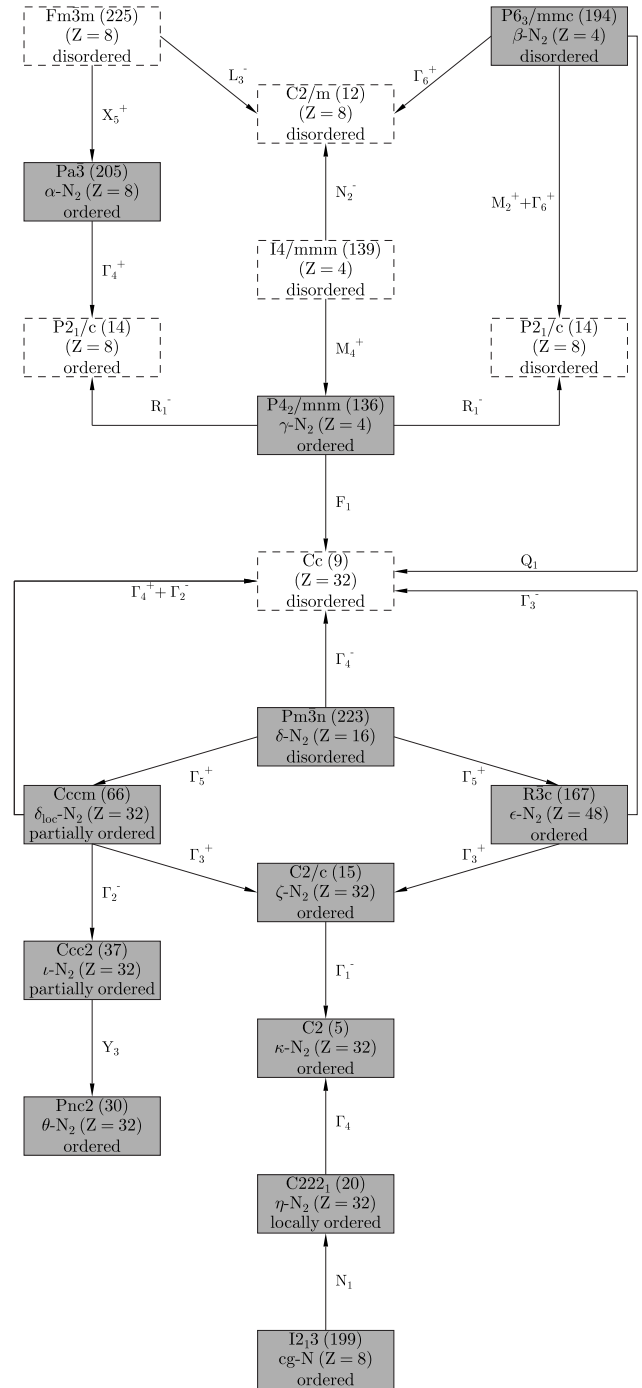


FIG. 10. Symmetry relationship between the structures of the different phases of nitrogen, assumed in our description. White boxes represent hypothetical structures assuming the role of intermediate, or parent, phases in the transition mechanisms. The irreducible representations associated with the symmetry-breaking order parameters are indicated along the lines relating the structures, following the notation of Stokes and Hatch (Ref. 29). The arrows are oriented from the parent higher-symmetry structure to the lower-symmetry structure.

mechanisms compatible with the rigid ellipsoid form of the N_2 molecules and preserving their small internuclear distance (1.0976 Å) compared to the intermolecular distance. The highly disruptive $\beta \rightarrow \alpha$ ordering results from a complex

transformation path via underlying disordered monoclinic ($C2/m$) and fcc intermediate stages. It is driven by the electric-quadrupole-quadrupole interaction,⁴³ associated with the prolate ellipsoidal charge distribution, whose contribution to the total intermolecular potential is minimized for the $Pa\bar{3}-\alpha$ molecular assembly. The ordered γ structure, which is formed either from β via a disordered tetragonal $I4/mmm$ substructure or from α with an intermediate ordered $P2_1/c$ structure, corresponds to a more efficient packing of ellipsoidal molecules on a tetragonal lattice, over-riding the quadrupolar effect.

Order-disorder structural transitions in the solid state display generally a second-order or weakly first-order character and preserve a group-subgroup relationship between the phase symmetries.⁴⁴ This is not the case for the transitions occurring in the low-pressure region of the phase diagram of nitrogen where, due to the high rigidity of the molecular units and weakness of the intermolecular interactions, the ordering processes involve very large strains and substantial atomic displacements leading to a loss of the group-subgroup relationship between adjacent structures. Our proposed $\beta \rightarrow \alpha$ and $\beta \rightarrow \gamma$ transition mechanisms require shear strains e_{xz} corresponding to a decrease in the monoclinic angle β in the common $C2/m$ intermediate substructure, by not less than 19.471° and 14.483° , respectively, and molecular displacements of about 1/12 of the intermolecular distances.

The drastic change observed for the transition mechanisms in region 2 with respect to region 1 reflects a simultaneous weakening of the intramolecular bonding and increase in the intermolecular interactions which constrain the molecular rotations. The importance of the anisotropic part of the interaction potential has been pointed out in several works,^{36,39} showing that the anisotropic term is essential for the stabilization of the ϵ phase and influences the orientational behavior of the N_2 molecules in the δ phase. This gives rise at high temperature to structures with different degrees of mixed orientational disorder, as δ , δ_{loc} , and ι , whereas with decreasing temperature orientational disorder freezes out, becoming increasingly hindered until the molecules begin to orientationally localize along well-defined directions, and ordered structures with nonquadrupolar interactions (ϵ, ζ, κ) take place. The orientational disorder also decreases with increasing pressure as attested by the stabilization of the ordered ζ and θ phases.

All the phases in region 2 display closely connected structures, separated by weakly first-order or second-order transitions. This is attested by Raman-scattering experiments which reveal successive branching of existing vibronic modes.^{6,8,9,26} δ - N_2 is the parent structure in this wide intermediate region of the phase diagram, all the other structures being deduced by small distortions. Following our proposed symmetries for the δ_{loc} , ζ , κ , ι , and θ phases, all the assumed structures, except θ - N_2 , possess 16 atoms in their primitive unit cells and therefore correspond (see Fig. 10) to structural instabilities at the centers (Γ) of the respective Brillouin zones. Therefore, as indicated in Table I, one has either ferroelastic transitions, induced by shear-strain order parameters, or ferroelectric transitions leading to the polar κ , ι , and θ structures. Ferroelectric transitions are uncommonly found

at high pressure. If the symmetry of our proposed polar structures is confirmed, it would show that in nitrogen the Coulomb interaction between charges on different molecules has a substantial contribution to the interaction potential in the 80–140 GPa high-pressure region.

With increasing pressure, the $N\equiv N$ bonds weaken and the intramolecular and intermolecular interactions become comparable, leading to a molecular dissociation at about 125–140 GPa at room temperature. The molecular-to-monoatomic pressure-induced transition is a classical transformation of the solid state, which is usually explained by the property of localized electrons to acquire, at high pressures and high densities, high kinetic energy, itinerant electronic configurations becoming energetically preferable. In this respect the semiconducting η phase should take place on the way to the band-gap closure of a higher-pressure metallic state.

In nitrogen the molecular dissociation is achieved only above 2000 K under the form of the cg phase built by strong N-N covalent bonds.¹⁰ In contrast the observations reported for the η phase can be interpreted as reflecting successive stages of the molecular dissociation. Our proposed η structure with local $C222_1$ symmetry, differing from the $Immm$ structure suggested by Caracas and Hemley,⁴² assumes a continuity in the symmetry-breaking mechanisms relating the highest-pressure molecular phases ζ and κ to the cg structure. The local arrangement of nitrogen atoms in the η phase seems to be preserved in the amorphization process, as attested by the closely related cg structure. A number of features of this process are reminiscent of a recent theoretical model proposed for the formation of amorphous solids.⁴⁵ In this model the amorphous state is described as the elastic analog of the mixed state of type II superconductors and shown to possibly recrystallize under pressure into a superhard state, which constitutes the elastic analog of the superconducting state. The very high bulk modulus, larger than 300 GPa, found for the recrystallized cg phase,¹⁴ to be compared with 443 GPa for diamond, clearly denotes ultrahard properties. Along the same line, one can speculate that the color changes observed on heating in the amorphous η phase reflect the decrease in density of elastic vortices formed by defect lines involving the remaining triple- or double-bonded nitrogen molecules.

The similarity between the cg phase of nitrogen and the diamond phase of carbon is not restricted to their ultrahard property. Mukherjee and Boehler²² pointed out that the negative slope of the melting curve found above 50 GPa and 1920 K in nitrogen can be compared with the decrease in the melting line in carbon, which starts at 5.6 GPa and 4790 K down to the graphite-diamond-liquid triple point at 9.4 GPa and 4300 K.^{46,47} The existence of a solid- N_2 -solid-polymeric-liquid triple point is extrapolated by Mukherjee and Boehler²² at 110 GPa and 1000 K. Other analogous properties between cg-N and diamond are the sharp drop in volume observed at the $\eta \rightarrow$ cg transition (22%),¹³ which is of the same order of magnitude than the 27% volume change found at 10 GPa for the graphite \rightarrow diamond transition,⁴⁷ and the large activation barrier toward the reverse transformation, cg-N being found to remain metastable down to 42 GPa.¹³ The reminiscence of the high-

pressure polymorphism of the group Va elements P, As, Sb, and Bi with the polymorphism of the IVa elements Si and Ge was recently stressed.⁴⁸ The similarity between cg-N and diamond shows that the structural continuity in the polymorphism of the two groups is not fortuitous even though they have different bonded properties at low pressure. This similarity derives from their electronic structures. In the s^2p^3 electronic configuration of nitrogen, which gives rise to its strong chemical bonding, the absence of $1p$ electrons allows the $2p$ valence electrons to closely approach the nucleus, while in the diamond structure the absence of p -electron states in the $1s^2$ atomic core allows the strongly p -character sp^3 bonding electrons to be held close to the nucleus. This latter property explains the extreme stability of the diamond structure and the singularity of the phase diagram of carbon,⁴⁹ compared to the rich polymorphism found for the other group IVa elements.⁵⁰ Analogously, the phase diagram of nitrogen is unique among group Va elements due to the extreme stability of its molecular units.

IV. SUMMARY AND CONCLUSION

In summary, structural mechanisms have been described for the pressure- and temperature-induced phase transitions in nitrogen. Three regions of the phase diagram have been distinguished, corresponding to different types of transition mechanisms and parent structures. Combined ordering and displacive reconstructive mechanisms take place in the lowest-pressure region 1, from the hexagonal β parent structure, whereas group-subgroup related structures are found in region 2, corresponding to slight distortions of the cubic δ parent structure. Molecular-to-atomic reconstructive transitions occurring in the more recently explored highest-pressure region 3 reflect the early stages of the dissociation process. Space-group symmetries, consistent with the assumed mechanisms, have been proposed for the δ_{loc} , ζ , κ , ι , and θ molecular phases and for the local structure of the amorphous η phase.

An analogy between the amorphous η to superhard cg transition and the vortex state to superconducting transition of type II superconductors has been emphasized. A verification of this analogy would require more detailed observations on the local structure of the η phase and on its evolution as a function of temperature and pressure. As noted in Ref. 45, at variance with superconducting vortices, amorphous elastic vortices are nondirectional and the corresponding defect lines can be formed, for example, by Somigliana type of dislocations,⁵¹ as suggested for glassy polymers⁵² and observed in damaged layers of amorphous silicon,⁵³ or by screw dislocations with variable Burgers vectors.⁵⁴ In this respect, the evolution observed with increasing temperature in the color of the η phase (from brownish-grayish to reddish) may reflect a progressive decrease in the density of vortices down to an almost single vortex state before the onset of the superhard cg phase.

APPENDIX

Let us illustrate our theoretical approach by describing explicitly the procedure used for two examples of transitions occurring in nitrogen.

1. Transition mechanism leading to the unknown structure of $\delta_{\text{loc}}\text{-N}_2$

Experimental observations^{5,25,26} show that $\delta_{\text{loc}}\text{-N}_2$ represents an intermediate, partially ordered, structure between the disordered $\delta\text{-N}_2$ and ordered $\epsilon\text{-N}_2$ structures. They also indicate that δ_{loc} and ϵ correspond to slight distortions of the cubic δ structure, with the same number of atoms [Eq. (16)] in their primitive unit cells. Group-theoretical considerations^{55,56} show that the $\delta (Pm\bar{3}n) \rightarrow \epsilon (R\bar{3}c)$ symmetry change is induced by the (IR) denoted Γ_5^+ in the Stokes-Hatch tables,²⁹ corresponding to a three-dimensional order parameter formed by the shear-strain components e_{xz} , e_{yz} , and e_{xy} , which yields the Landau free energy,^{29,55,56}

$$F_1(T, P, e_{ij}) = a_1(e_{xz}^2 + e_{yz}^2 + e_{xy}^2) + a_2e_{xz}e_{yz}e_{xy} + a_3(e_{xz}^4 + e_{yz}^4 + e_{xy}^4) + \dots \quad (\text{A1})$$

When F is truncated at the fourth degree its minimization with respect to the shear components yields three possible stable states^{29,57} corresponding to the following subgroups of $Pm\bar{3}n$: (I) $R\bar{3}c$ for $e_{xz}=e_{yz}=e_{xy} \neq 0$, which coincides with the $\epsilon\text{-N}_2$ symmetry, (II) $Cccm$ for $e_{xz} \neq 0$, $e_{yz}=e_{xy}=0$, and (III) $C2/c$ for $e_{xz} \neq 0$, $e_{yz}=e_{xy} \neq 0$. Due to the existence of a non-vanishing cubic a_2 invariant in F , the transitions to states I and III are necessarily first order, whereas the vanishing of the cubic invariant allows the $Pm\bar{3}n \rightarrow Cccm$ transition to be possibly second order *as it is observed experimentally for the $\delta \rightarrow \delta_{\text{loc}}$ transition.*^{5,25} Accordingly, one can reasonably assume a $Cccm$ ($Z=16$) symmetry for the δ_{loc} phase. A realistic structural model for this phase has to fulfill the following requirements. (1) It involves a partial orientational ordering of the disklike and spherelike molecules with respect to the fully disordered $\delta\text{-N}_2$ structure,^{4,25} compatible with the $Cccm$ symmetry. (2) Since the $\delta \rightarrow \epsilon$ transition involves small displacements of the N_2 molecules accompanied by a slight extension of the lattice along the cube diagonal, resulting in a shift of less than 5° in the angle between axes,⁴ the atomic positions in $\delta_{\text{loc}}\text{-N}_2$ should be intermediate between the δ and ϵ positions. In $\delta\text{-N}_2$ ($a=6.164 \text{ \AA}$) nitrogen atoms occupy the Wyckoff positions $16i$ (0.542 0.542 0.542) and $48l$ (0.739 0.031 0.580), whereas in $\epsilon\text{-N}_2$ ($a=5.928 \text{ \AA}$, $\alpha=85.14^\circ$) the atoms are in positions $4c$ (0.0495 0.0495 0.0495) and $12f$ (0.7224 0.0559 0.5701). The δ_{loc} pseudotetragonal unit cell described in Fig. 5(b) constitutes the most compatible structure fulfilling the preceding requirements.

2. $\alpha \rightarrow \gamma$ reconstructive transition

The determination of the transition path between two structures A and B separated by a reconstructive transition, with no group-subgroup relationship between their space-group symmetries, has been described in a number of works (see, for example, Refs. 57–60). It consists of (1) finding the substructures corresponding to the maximal common subgroups of the A and B space groups, (2) determining the transition paths going across the preceding substructures in term of collective displacements and strains, and (3) selecting among the preceding paths the one involving the shortest set of displacements and minimal strains. A number of inter-

TABLE II. Possible transition paths for the $\alpha \rightarrow \gamma$ phase transition in nitrogen. Each path is defined by a common subgroup of both the α and γ structures. For each transition path the lattice translations, the origin shift, the lattice parameters, and the atomic positions in the setting of the common subgroup and the maximal atomic displacements are given.

TP	Space group	Subgroup	Lattice translations	Origin shift	Lattice parameters				Atomic positions			Shifts (Å)	
1	$P\bar{a}3$	$P2_1/c$	(0,0,1),(1,0,0),(0,1,0)	(0,0,0)	5.667	5.667	5.667	90	4e	0.0550	0.0550	0.0550	0.5
		$P4_2/mnm$	(0,0,-1),(-1,-1,0),(-1,1,0)	(-1/2,-1/2,-1/2)	5.109	5.596	5.596	90	4e	0.0000	0.0000	0.0950	
2	$P\bar{a}3$	$P2_1/c$	(0,1,0),(0,0,1),(1,0,0)	(0,0,0)	5.667	5.667	5.667	90	4e	0.0550	0.0550	0.0550	0.7
		$P4_2/mnm$	(0,-1,1),(-1,0,0),(0,-1,-1)	(0,0,0)	6.462	3.957	6.462	104.48	4e	0.0475	0.0950	0.0475	
3	$P\bar{a}3$	$P2_1/c$	(0,1,0),(0,0,1),(1,0,0)	(0,0,0)	5.667	5.667	5.667	90	4e	0.0550	0.0550	0.0550	0.8
		$P4_2/mnm$	(0,-1,1),(-1,0,0),(0,-1,-1)	(-1/2,-1/2,-1/2)	6.462	3.957	6.462	104.48	4e	0.0475	0.0950	0.0475	
									4e	0.5475	0.9050	0.5475	

mediate substructures can be found, which are common to the α -N₂ ($P\bar{a}3$, $Z=8$) and γ -N₂ ($P4_2/mnm$, $Z=4$) structures. Among these the monoclinic substructure with the space group $P2_1/c$ ($Z=8$) displays the highest symmetry and the smallest number of atoms in the primitive unit cell. The transition path $\alpha \rightarrow P2_1/c \rightarrow \gamma$ involves two IRs, denoted Γ_4^+ and R_1^- in the notation of Stokes and Hatch,²⁹ associated, respectively, with the hypothetical, group-subgroup related, transitions $P\bar{a}3 \rightarrow P2_1/c$ and $P4_2/mnm \rightarrow P2_1/c$. The cubic-to-monoclinic transition corresponds to the same free energy F_1 given by Eq. (A1), the $P2_1/c$ structure being stabilized for $e_{xz} \neq 0$, $e_{xy} = e_{yz} = 0$. The order parameter describing the tetragonal-to-monoclinic transition has four components, denoted $\eta_1 - \eta_4$ which gives rise to the Landau free energy restricted at the fourth degree,

$$F_2(T, P, \eta_i) = b_1(\eta_1^2 + \eta_2^2 + \eta_3^2 + \eta_4^2) + b_2(\eta_1^2 \eta_2^2 + \eta_3^2 \eta_4^2) + b_3(\eta_1^2 \eta_3^2 + \eta_2^2 \eta_4^2) + b_4(\eta_1^2 \eta_4^2 + \eta_2^2 \eta_3^2). \quad (\text{A2})$$

Minimization of F_2 shows that the $P2_1/c$ structure is stabi-

lized for $\eta_1 = \eta_3 \neq 0$, $\eta_2 = \eta_4 = 0$. In order to determine the effective transition path followed at the $\alpha \rightarrow \gamma$ transition one has to consider the atomic positions in the two structures. In α -N₂ the nitrogen atoms occupy the Wyckoff positions $8c$ (0.055 0.055 0.055) with the molecule centers in position $4a$ (0 0 0). In γ -N₂ the atoms occupy the positions $4f$ (0.095 0.095 0.000), with the molecule centers at $2a$ (0 0 0). Table II indicates the atomic shifts associated with the different possible transition paths relating the α and γ structures when going across a monoclinic $P2_1/c$ intermediate substructure, taking into account the reorientation of the N₂ molecules from the cube to the square diagonals. The effective transition path, represented in Fig. 4, corresponds to the shortest atomic shifts (0.5 Å) involving the minimal shear strain e_{xz} . One can then verify that other intermediate substructures with lower symmetries (Pc , $P\bar{1}$) or more than eight atoms in the primitive cell correspond to larger atomic shifts and strains.

*hanne@min.uni-kiel.de

¹D. A. Young, *Phase Diagrams of the Elements* (University of California Press, Berkeley, 1991).

²T. A. Scott, Phys. Rep., Phys. Lett. **27**, 89 (1976).

³B. Olinger, J. Chem. Phys. **80**, 1309 (1984).

⁴R. L. Mills, B. Olinger, and D. T. Cromer, J. Chem. Phys. **84**, 2837 (1986).

⁵M. I. M. Scheerboom and J. A. Schouten, Phys. Rev. Lett. **71**, 2252 (1993).

⁶R. Bini, M. Jordan, L. Ulivi, and H. J. Jodl, J. Chem. Phys. **108**,

6849 (1998).

⁷R. Bini, L. Ulivi, J. Kreutz, and H. J. Jodl, J. Chem. Phys. **112**, 8522 (2000).

⁸E. Gregoryanz, A. F. Goncharov, C. Sanloup, M. Somayazulu, H.-K. Mao, and R. J. Hemley, J. Chem. Phys. **126**, 184505 (2007).

⁹E. Gregoryanz, A. F. Goncharov, R. J. Hemley, and H. K. Mao, Phys. Rev. B **66**, 224108 (2002).

¹⁰A. F. Goncharov, E. A. Gregoryanz, H.-K. Mao, Z. Liu, and R. J. Hemley, Phys. Rev. Lett. **85**, 1262 (2000).

- ¹¹M. I. Eremets, R. J. Hemley, H.-K. Mao, and E. Gregoryanz, *Nature (London)* **411**, 170 (2001).
- ¹²E. Gregoryanz, A. F. Goncharov, R. J. Hemley, and H.-K. Mao, *Phys. Rev. B* **64**, 052103 (2001).
- ¹³M. I. Eremets, A. G. Gavriliuk, N. R. Serebryanaya, I. A. Trojan, D. A. Dzivenko, R. Boehler, H.-K. Mao, and R. J. Hemley, *J. Chem. Phys.* **121**, 11296 (2004).
- ¹⁴M. I. Eremets, A. G. Gavriliuk, I. A. Trojan, D. A. Dzivenko, and R. Boehler, *Nat. Mater.* **3**, 558 (2004).
- ¹⁵M. I. Eremets, A. G. Gavriliuk, and I. A. Trojan, *Appl. Phys. Lett.* **90**, 171904 (2007).
- ¹⁶M. L. Vos and J. A. Schouten, *J. Chem. Phys.* **91**, 6302 (1989).
- ¹⁷C. A. Swenson, *J. Chem. Phys.* **23**, 1963 (1955).
- ¹⁸B. M. Powell, G. Dolling, and H. F. Nieman, *J. Chem. Phys.* **79**, 982 (1983).
- ¹⁹J. Donohue, *The Structures of the Elements* (Wiley, New York, 1974).
- ²⁰A. F. Schuch and R. L. Mills, *J. Chem. Phys.* **52**, 6000 (1970).
- ²¹D. A. Young, C. S. Zha, R. Boehler, J. Yen, M. Nicol, A. S. Zinn, D. Schiferl, S. Kinkead, R. C. Hanson, and D. A. Pinnick, *Phys. Rev. B* **35**, 5353 (1987).
- ²²G. D. Mukherjee and R. Boehler, *Phys. Rev. Lett.* **99**, 225701 (2007).
- ²³D. T. Cromer, R. L. Mills, D. Schiferl, and L. Schwalbe, *Acta Crystallogr., Sect. B: Struct. Crystallogr. Cryst. Chem.* **37**, 8 (1981).
- ²⁴H. Olijnyk, *J. Chem. Phys.* **93**, 8968 (1990).
- ²⁵M. I. M. Scheerboom and J. A. Schouten, *J. Chem. Phys.* **105**, 2553 (1996).
- ²⁶L. Tassini, F. Gorelli, and L. Ulivi, *J. Chem. Phys.* **122**, 074701 (2005).
- ²⁷M. Hanfland, M. Lorenzen, C. Wassilew-Reul, and F. Zoutone, *Rev. High Pressure Sci. Technol.* **6**, 130 (1997).
- ²⁸M. J. Lipp, J. P. Klepeis, B. J. Baer, H. Cynn, W. J. Evans, V. Iota, and C. S. Yoo, *Phys. Rev. B* **76**, 014113 (2007).
- ²⁹H. T. Stokes and D. M. Hatch, *Isotropy Space Groups of the 230 Crystallographic Space Groups* (World Scientific, Singapore, 1988).
- ³⁰B. C. Kohin, *J. Chem. Phys.* **49**, 2898 (1971).
- ³¹D. A. Goodings and M. Henkelmann, *Can. J. Phys.* **49**, 2898 (1971).
- ³²S. Nosé and M. L. Klein, *Phys. Rev. Lett.* **50**, 1207 (1983).
- ³³A. K. McMahan and R. LeSar, *Phys. Rev. Lett.* **54**, 1929 (1985).
- ³⁴R. D. Ethers, V. Chandrasekharan, E. Uzan, and K. Kobashi, *Phys. Rev. B* **33**, 8615 (1986).
- ³⁵H. B. Radousky, W. J. Nellis, M. Ross, D. C. Hamilton, and A. C. Mitchell, *Phys. Rev. Lett.* **57**, 2419 (1986).
- ³⁶J. Belak, R. LeSar, and R. D. Ethers, *J. Chem. Phys.* **92**, 5430 (1990).
- ³⁷C. Mailhiot, L. H. Yang, and A. K. McMahan, *Phys. Rev. B* **46**, 14419 (1992).
- ³⁸T. W. Barbee III, *Phys. Rev. B* **48**, 9327 (1993).
- ³⁹A. Mulder, J. P. J. Michels, and J. A. Schouten, *Phys. Rev. B* **57**, 7571 (1998).
- ⁴⁰W. D. Mattson, D. Sanchez-Portal, S. Chiesa, and R. M. Martin, *Phys. Rev. Lett.* **93**, 125501 (2004).
- ⁴¹S. Krukowski and P. Strak, *J. Chem. Phys.* **124**, 134501 (2006).
- ⁴²R. Caracas and R. J. Hemley, *Chem. Phys. Lett.* **442**, 65 (2007).
- ⁴³C. A. English and J. A. Venables, *Proc. R. Soc. London, Ser. A* **340**, 57 (1974).
- ⁴⁴N. G. Parsonage and L. A. K. Staveley, *Disorder in Crystals* (Clarendon, Oxford, 1978).
- ⁴⁵P. Tolédano, *Europhys. Lett.* **78**, 46003 (2007).
- ⁴⁶M. Togaya, *Phys. Rev. Lett.* **79**, 2474 (1997).
- ⁴⁷L. D. Son, G. M. Rusakov, and N. N. Katkov, *Dokl. Phys.* **51**, 56 (2006).
- ⁴⁸H. Katzke and P. Tolédano, *Phys. Rev. B* **77**, 024109 (2008).
- ⁴⁹H. Katzke, U. Bismayer, and P. Tolédano, *J. Phys.: Condens. Matter* **18**, 5129 (2006).
- ⁵⁰H. Katzke, U. Bismayer, and P. Tolédano, *Phys. Rev. B* **73**, 134105 (2006).
- ⁵¹J. C. M. Li, *Metall. Trans. A* **16**, 2227 (1985).
- ⁵²C. G'Sell, *Mater. Sci. Eng., A* **309-310**, 539 (2001).
- ⁵³M. Ishimaru, S. Harada, and T. Motooka, *J. Appl. Phys.* **81**, 1126 (1997).
- ⁵⁴P. Chaudhari, A. Levi, and P. Steinhardt, *Phys. Rev. Lett.* **43**, 1517 (1979).
- ⁵⁵J. C. Tolédano and P. Tolédano, *Phys. Rev. B* **21**, 1139 (1980).
- ⁵⁶J. C. Tolédano and P. Tolédano, *The Landau Theory of Phase Transitions* (World Scientific, Singapore, 1987).
- ⁵⁷P. Tolédano and V. Dmitriev, *Reconstructive Phase Transitions* (World Scientific, Singapore, 1996).
- ⁵⁸V. P. Dmitriev, S. B. Rochal, Yu. M. Gufan, and P. Tolédano, *Phys. Rev. Lett.* **60**, 1958 (1988).
- ⁵⁹O. Blaschko, V. Dmitriev, G. Krexner, and P. Tolédano, *Phys. Rev. B* **59**, 9095 (1999).
- ⁶⁰P. Tolédano, *Z. Kristallogr.* **220**, 672 (2005).